Global J. Environ. Sci. Manage. 9(3): 353-372, Summer 2023, Serial #35

Global Journal of Environmental Science and Management
(GJESM)

Homepage: https://www.gjesm.net/

Podcasts

CASE STUDY

Land surface temperature changes caused by land cover/ land use properties and their impact on rainfall characteristics

A. Suharyanto[1,*], A. Maulana[2], D. Suprayogo[3], Y.P. Devia[1], S. Kurniawan[3]

[1] *Civil Engineering Department, Universitas Brawijaya, Kota Malang, Indonesia*

[2] *Department of Geology, Universitas Hasanuddin, Gowa, Makassar, Indonesia*

[3] *Department of Soil Sciences, Universitas Brawijaya, Kota Malang, Indonesia*

ARTICLE INFO

Article History:
Received 27 May 2022
Revised 30 August 2022
Accepted 26 October2022

Keywords:
Image processing
Land surface temperature
Thiessen polygon
Vegetation index

ABSTRACT

BACKGROUND AND OBJECTIVES: This study aims to determine the relationships between land cover presented by vegetation index and land surface temperature, between vegetation index and the built-up index, between built-up index and land surface temperature, and between land surface temperature and rainfall characteristics in East Java Province, Indonesia.

METHODS: Three cities and four regencies were used as examples. Landsat imagery scanned in 1995, 2001, 2015, and 2020 were used. Daily rainfall data recorded in the same years with Landsat data are used. The pixel values along the urban heat island line were used to analyze the interrelationships between vegetation index, built-up index, and land surface temperature. The land surface temperature and daily rainfall data from each Thiessen polygon were used to analyze the relationship between land surface temperature and rainfall characteristics. Image processing analysis was used to analyze the vegetation index, built-up index, and land surface temperature. The mathematical interrelationship between vegetation index, built-up index, land surface temperature, and rainfall intensity was analyzed using linear regression.

FINDINGS: The results of the analysis show that the relationship between vegetation index and built-up index is inversely proportional and with land surface temperature is nearly inversely proportional to a coefficient of determination greater than 0.5. For the relationship between the built-up index and land surface temperature, the results of the analysis show that both have a directly proportional relationship, with a significant coefficient of determination (R2>0.5). For the relationship between land surface temperature and rainfall characteristics, the results of the analysis show that land surface temperature has a directly proportional but weak relationship with rainfall intensity and an inversely proportional but weak relationship with the number of rainfall days. Decreasing environmental conditions indicated by decreasing vegetation index will influence increasing land surface temperature and its effect on increasing rainfall intensity and decreasing rainfall days.

CONCLUSION: Changes in land use/land cover are characterized by a change in vegetation cover to built-up land. These changes affect the land surface temperature. Changes in land surface temperature affect the occurrences of rainfall intensity. When the vegetation index decreases, the built-up index increases, and the land surface temperature increases as well. The increase in land surface temperature will increase the rainfall intensity. Satellite remote sensing imagery is effective and efficient for analyzing vegetation index, built-up index, and land surface temperature.

DOI: 10.22035/gjesm.2023.03.01

NUMBER OF REFERENCES	NUMBER OF FIGURES	NUMBER OF TABLES
50	10	9

*Corresponding Author:
Email: *agus.s@ub.ac.id*
Phone: +62341 551430
ORCID: 0000-0002-1508-7685

Note: Discussion period for this manuscript open until October 1, 2023 on GJESM website at the “Show Article”.

INTRODUCTION

Population growth in Indonesia, particularly in East Java Province, follows the exponential function (BPS-SJTP, 2021; Nicolau *et al.,* 2018). Food, clothing, and household consumption increase rapidly to fulfill the basic needs of human life. To increase food production, agricultural land needs to be expanded. Agricultural land is located in flat areas but is currently being expanded to hilly areas. To meet the housing needs, the city grows from suburban areas, such as agricultural or forest areas, to urban areas. This activity are converted pervious areas into impervious areas. This phenomenon will rapidly change land use/land cover (LULC) from vegetation areas to non-vegetation areas (Moslenko *et al.,* 2020; Stehfest *et al.,* 2019), which will affect the increase of the land surface temperature (LST) (Guha *et al.,* 2018; Hua and Ping, 2018). Garouani *et al*. (2021) concluded that LULC change has an important consequence in hydrology. Predicting precipitation until the 21century is affected by LST (Himayoun *et al*, 2020). Hu *et al*. (2020) mentioned that trend surface runoff has consistent with the trend of impervious area, and Shiraki and Shigeta (2013) was concluded there is a relation between LST and convective precipitation frequency. From those studied, no discussion of the relationship between LST and rainfall intensity and the number of rainfall days (NRD). The rainfall characteristics are important as input data to peak discharge analysis. The peak discharge data are most important in flood analysis, water structure design, and soil erosion analysis (Anache *et al.,* 2017; Kovář *et al.,* 2012; Jiang *et al.,* 2019; Mapiam *et al.,* 2014). In this study, the effect of LST on the rainfall characteristics especially in rainfall intensity and NRD needs to be evaluated. Satellite remote sensing data are one of the powerful data used to analyze the LULC change from vegetation areas to non-vegetation areas and LST change (Derdouri *et al.,* 2021; Ferrelli *et al.,* 2018). One of them is Landsat imagery data. LULC change can be analyzed using multi-spatial and multi-temporal satellite remote sensing data. The normalized difference vegetation index (NDVI) is one of the vegetation indices commonly used to analyze plant greenness (Mondino *et al.,* 2016; Turvey and McLaurin, 2012). The value of NDVI ranges from −1 to + 1. Values between 0 and −1 indicate that the land is covered by non-vegetation objects, such as dead plants, stones, roads, houses, and barren land. The degree or level of land covered by green foliage or plants is indicated by the NDVI with values from 0 to +1 (Chang *et al.,* 2021; Reid *et al.,* 2018). Zero indicates the lowest area covered by green foliage or plants, and +1 indicates the highest area covered by green foliage or plants. In previous studies, many researchers concluded that LST is related to the pattern of LULC change, such as urbanized, vegetation, and water areas (Almouctar, 2021; Maselli, 2012; Samal and Gedam, 2017). Here the LULC change can be represented by the change of NDVI. The plant greenness will determine the level of solar radiation absorbed by the leaves. The area with a high level of plant greenness, which is indicated by the NDVI value of +1, will have an LST lower than that of the area with a low level of plant greenness. The relationship between NDVI and LST will be discussed as the first objective of this study. The LULC change can also be indicated by the change of the normalized difference built-up index (NDBI). This index indicates the level of the built-up area, particularly in the urbanized area (Badlani *et al.,* 2017; Ibrahim, 2017). NDBI is the opposite of NDVI. NDBI indicates the built-up area (impervious area), including barren land, whereas NDVI indicates land covered by green foliage or plants, including vegetation, agricultural land, parks, and gardens, as well as open space. The relationship between NDVI and NDBI can be predicted to have a negative correlation. This phenomenon will also be discussed as the second objective of this study. Climate change is one of the phenomena that should be considered in the civil work plan. One of the climate change indicators is the increase of LST. Devi *et al*. (2020) concluded that deforestation has an effect on LST, and Liu *et al*. (2021) mentioned that LST change varied over different regions. A high LST and a low NDVI will affect the decrease of rainfall and soil moisture (Shiraki and Shigeta, 2013). Compared with LST, land elevation has a more significant effect on increasing the frequency of convective rainfall than surface temperature (Peng *et al.,* 2020; Shiraki and Shigeta, 2013). The relationship between LST and rainfall characteristics needs to be analyzed, and it is the third objective of this work. East Java Province, Indonesia is one of the provinces in Indonesia with rapid LULC change (BPS-SJTP, 2021; Indarto and Hakim, 2021). The second largest city in Indonesia, i.e., Surabaya City, is located in East Java Province. As the second largest city, the development of Surabaya

City is fast, and LULC change is occurring rapidly (BPS-SSM, 2021). A well-known resort area, i.e., Batu City, is located in East Java Province. This city was established in 2004, and LULC change is occurring rapidly. Under these conditions, the LULC change represented by NDVI and its effect on the LST and rainfall characteristics in the aforementioned areas need to be analyzed. The study will be conducted in three cities and four regencies in East Java Province. The Landsat Thematic Mapper (TM), Enhanced Thematic Mapper (ETM+), and Operational Land Imager (OLI) imageries recorded in 1995, 2000, 2015, and 2020 are used in this study. Daily rainfall in the same years recorded at the rainfall stations located surrounding each study area is used as input data in the analysis of the relationship between LST and rainfall characteristics. Three analyses i.e., relationship between NDVI and LST, between NDVI and NDBI, and between LST and rainfall characteristics will be analyzed in this study. Given that climate change is occurring rapidly, research on the effects of LULC change represented by NDVI on the LST, NDBI, and rainfall characteristics in East Java Province needs to be conducted. The main contribution of this study is to quantitatively analyze the LULC change in some areas in East Java Province from 1995 to 2020 using multi-temporal Landsat imagery. The main purpose of this study is to determine the relationship between LULC change and rainfall characteristics. It can be expected that the results of this study can be implemented to predict the rainfall characteristics based on LULC change, particularly in East Java Province. This study has been carried out in East Java Province Indonesia with 3 cities and 4 regencies in the years 1995, 2001, 2015, and 2020.

MATERIALS AND METHODS

Study area

The study area is three cities and four regencies in East Java Province, Indonesia. The three cities are Surabaya, Malang, and Batu. Surabaya City is located in a lowland area with a flat topography with an elevation of 3–6 meters (m) above sea level and bounded by sea and land. Malang and Batu cities are located in a hilly area and bounded by land. The elevation of Malang City is 445–526 m above sea level, and the average elevation of Batu City is 897 m above sea level. The four regencies are Malang, Probolinggo, Sampang, and Tuban. Malang Regency is located in the southern part of East Java Province, and its southern area is facing the Indian Ocean. The elevation of Malang Regency is 0–3,600 m above sea level. Probolinggo Regency is located in the middle of East Java Province, and its northern area is facing the Madura Strait. The elevation of Probolinggo Regency is 0–1,500 m above sea level. Across Probolinggo Regency is Sampang Regency. Sampang Regency is located in the middle of Madura Island, and its southern area is facing the Madura Strait and its northern area is facing the Java Sea. The elevation of the Sampang Regency is 0–375 m above sea level. Tuban Regency is located in the western part of East Java Province, and its northern area is facing the Java Sea. The elevation of Tuban Regency is 0–500 m above sea level. A summary of the geographical and demographic conditions of the study area is shown in Table 1. Based on these conditions, Surabaya City represents a high-density population and lowland area, and Malang and Batu cities represent hilly areas and growing cities. Meanwhile, Malang Regency represents areas located in the southern part of East Java Province, Probolinggo Regency represents areas located in the middle part of East Java Province, Sampang Regency represents areas located in the middle of Madura Island, and Tuban Regency represents areas located in the northern part of East Java Province. The location of the study area is shown in Fig. 1. The aims of the current study can be summarized as: 1) To explore the LULC changes represented by NDVI, NDBI, and LST from Landsat imageries data; 2) To understand interrelationships between NDVI, NDBI, and LST; and 3) To find the

Table 1: Geographic and demographic conditions of the study locations

No.	Location	Area (km^2)	Population	Topography
1.	Batu City	199.09	213.046	Hilly
2.	Malang City	110.06	843.810	Hilly
3.	Surabaya City	326.81	2,970,000	Flat
4.	Malang Regency	3,530.65	2,654,448	Flat–mountainous
5,	Probolinggo Regency	1,696.17	1,152,537	Flat–mountainous
6.	Sampang Regency	1,233.30	969,694	Flat–hilly
7.	Tuban Regency	1,839.94	1,198,012	Flat–hilly

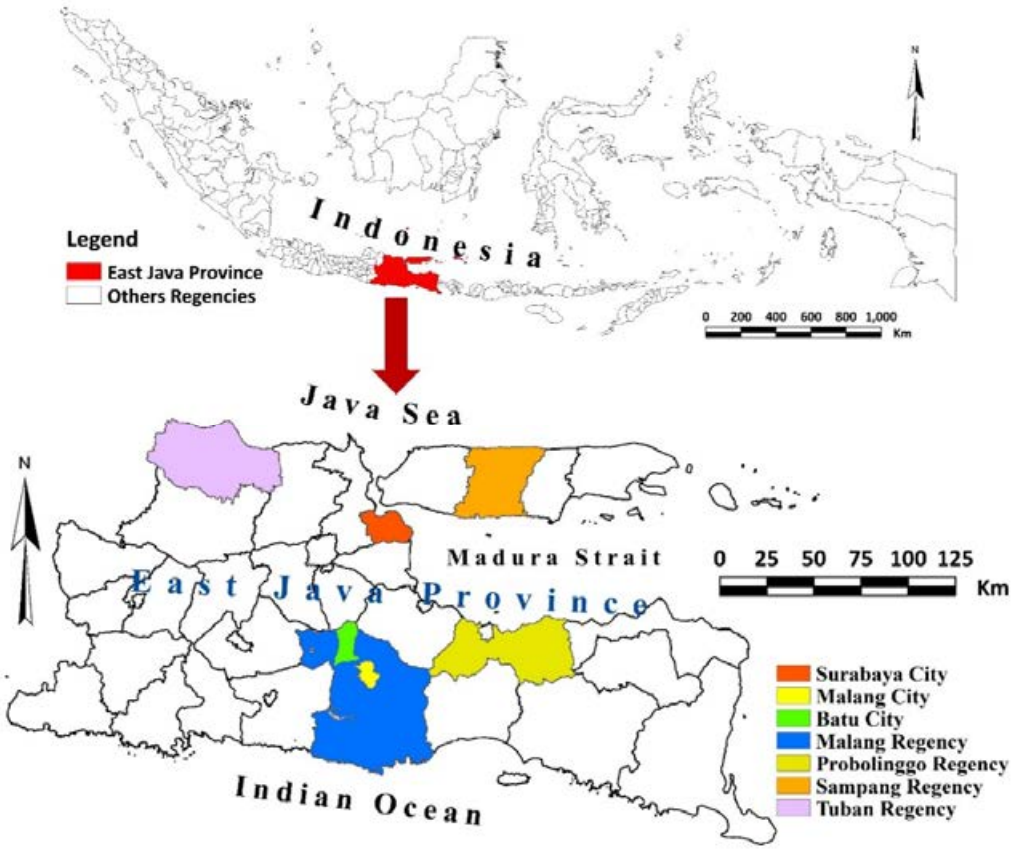

Fig. 1: Geographic location of the study area in East Java Province, Indonesia

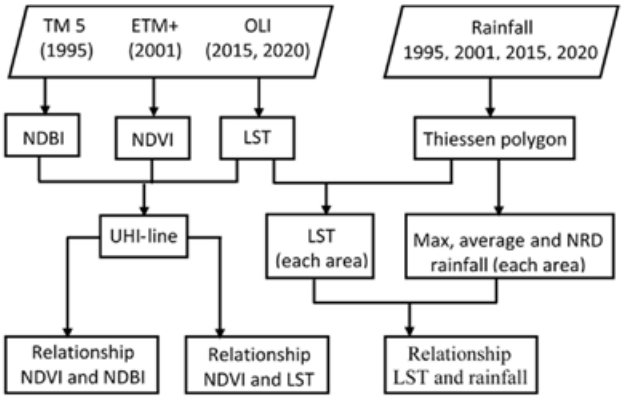

Fig. 2: Flow diagram of the study method

relationship between LST and rainfall characteristics.

In principle, the methodology used in this study includes image processing, rainfall data analysis using the Thiessen polygon method, and regression analysis. The diagram of the overall methodology used in this study is shown in Fig. 2.

Image processing

Many satellites are recording the earth's surface conditions. Among them is Landsat. The Landsat satellite is equipped with the TM, ETM+, and OLI sensors to scan the earth's surface conditions. The imageries scanned by these sensors are used in this

research. Image processing was conducted to achieve the study goals, which include determining the NDVI, LST, urban heat island (UHI), and NDBI. NDVI indicates the LULC change based on the greenness level in the study area. The Geographic Information System (GIS) software was used for image processing.

Extraction of NDVI

NDVI is calculated based on the ratio of visible to near-infrared (NIR) light absorbed and reflected by plants. For Landsat 5 TM and Landsat 7 ETM+, visible and NIR light are recorded at Bands 3 and 4, and for Landsat 8 OLI, visible and NIR light are recorded at Bands 4 and 5. The value of NDVI ranges from −1 to +1. The values from −1 to 0 indicate that the area is covered by dead plants, rock, water, bare land, and built-up areas (Ozyavuz *et al.,* 2015). The NDVI values ranging from 0 to 0.33 indicate unhealthy plants, 0.33 to 0.66 indicate moderately healthy plants, and 0.66 to 1 indicate very healthy plants (Chen *et al.,* 2021). The formula used to calculate the NDVI values for Landsat TM and ETM+ is expressed in Eq. 1 (Osyavus *et al.,* 2015), and the formula used to calculate the NDVI value for Landsat 8 OLI, using Eq. 2 (Chang *et al.,* 2021).

$$\text{NDVI} = (\text{Band 4} - \text{Band 3})/(\text{Band 4} + \text{Band 3}) \quad (1)$$

$$\text{NDVI} = (\text{Band 5} - \text{Band 4})/(\text{Band 5} + \text{Band 4}) \quad (2)$$

Extraction of NDBI

In principle, urbanization is the change of land cover from pervious areas to impervious areas caused by the overlay of the land surface by impervious materials, such as concrete, asphalt, and roof. One indicator that can be used to detect the urbanization rate is NDBI, which is generated from satellite images. The formula used to calculate the NDBI is expressed in Eq. 3 (Badlani *et al.,* 2017; Bonafoni *et al.,* 2016). For Landsat TM and ETM+, short wave infrared (SWIR) and NIR are represented by Bands 5 and 4, respectively. For Landsat 8 OLI, SWIR and NIR are represented by Bands 6 and 5, respectively. The value of NDBI ranges between −1 and +1. A large NDBI value indicates that the area has large proportions of built-up and construction areas (Firozjaei *et al.,* 2019).

$$\text{NDBI} = (\text{SWIR} - \text{NIR})/(\text{SWIR} + \text{NIR}) \quad (3)$$

Extraction of LST from Landsat TM, ETM+, and OLI

LST is a natural phenomenon that can be detected using satellite remote sensing data. For Landsat 5 TM and Landsat 7 ETM+, LST can be generated from Band 6. For Landsat 8 OLI, LST is analyzed using Band 10 or 11. The formula used to calculate LST from Landsat TM and ETM is expressed using Eq. 4 (Grover and Singh, 2015; Mustafa *et al.,* 2020; Ranagalage *et al.,* 2017).

$$L_\lambda = ((L_{max\lambda} - L_{min\lambda})/(QCAL_{max} - QCAL_{min}))*((QCAL - QCAL_{min}) + L_{min\lambda}), \quad (4)$$

Where, L_λ is the temperature of the satellite sensor (brightness radiance), $L_{max\lambda}$ is the maximum radiance, $L_{min\lambda}$ is the minimum radiance, $QCAL_{max}$ is the quantized calibrated maximum, $QCAL_{min}$ is the quantized calibrated minimum, and *QCAL* is the digital number (DN) of Band 6. Based on the brightness radiance, LST can be calculated using Eq. 5 (Almeida *et al.,* 2021).

$$T = \frac{K_2}{\ln\left(\frac{K_1}{L_{\ddot{e}}} + 1\right)} \quad (5)$$

Where, T is the LST (Kelvin), K_1 is Constant 1, and K_2 is Constant 2. The values of K_1 and K_2 can be found in the Landsat 7 (L7) Data Users Handbook (USGS, 2019). To convert the LST from degrees Kelvin to degrees Celsius, 273.15 should be subtracted from *T,* using Eq. 6 (Grover and Singh, 2015).

$$TC = T - 273.15 \quad (6)$$

Where, *TC* is the LST in degrees Celsius.

For Landsat 8 OLI, the calculation to determine the LST can be done as follows. The first step is to calculate the top of atmospheric (TOA) spectral radiance, using Eq. 7 (Hua and Ping, 2018).

$$TOA = M_L * C_{cal} + A_L, \quad (7)$$

Where, M_L is the radiance multiplicative scaling factor (Radiance_Mult_Band_10) obtained from the MTL file on the Landsat data, A_L is the radiance

additive scaling factor (Radiance_Add_Band_10) obtained from the MTL file on the Landsat data, and C_{cal} is the digital value of Band 10. *TOA* can also be calculated using the same equation expressed in Eq. 6.

The second step is to calculate the brightness temperature in degrees Celsius, using Eq. 8 (Garouani *et al.,* 2021).

$$\mathrm{TC} = \frac{K_2}{\ln\left(\frac{K_1}{L_\lambda} + 1\right)} - 273.15. \tag{8}$$

For Landsat 8 OLI, K_1 and K_2 are the band-specific thermal conversion constants taken from the metadata of the imagery file.

The third step is to calculate the proportional vegetation (PV) using the NDVI, as expressed as Eq. 9 (Alexander, 2020).

$$\mathrm{PV} = \left(\frac{\mathrm{NDVI} - \mathrm{NDVI}_{\min}}{\mathrm{NDVI}_{\max} - \mathrm{NDVI}_{\min}}\right)^2 \tag{9}$$

The fourth step is to calculate the error correction (*E*), using Eq. 10 (Guha *et al.,* 2018).

$$E = 0.004 * PV + 0.986. \tag{10}$$

The fifth step is to calculate the LST in degrees Celsius, using Eq. 11 (Ranagalage *et al.,* 2017).

$$\mathrm{LST} = \frac{\mathrm{TC}}{\left\{1 + \left[\left(\lambda \mathrm{TC}/\rho\right) \mathrm{Ln}E\right]\right\}}, \tag{11}$$

Where, λ is the DN of Band 10 (λ is the wavelength of emitted radiance (λ = 11.5 µm for Landsat TM Band 6, λ = 10.8 µm for Landsat TIRS Band 10) [Senanayake *et al.,* 2013], ρ = 14,380 ($\rho = h \times c/\sigma$ (1.438×10^{-2} mK)), *TC* is the brightness temperature, σ is the Boltzmann constant (1.38×10^{-23} J/K), *h* is the Planck constant (6.626×10^{-34} Js), *c* is the velocity of light (2.998×10^{8} m/s), and *E* is the land surface emissivity or error correction.

Analyses of UHI

The analysis of the LST is associated with the UHI phenomenon. The UHI is part of the LST located at the center of an urbanized area and depends on where the line of the UHI will be drawn in the study area (Almeida *et al.,* 2021). Normally, the line of the UHI is initially drawn from a suburban area to an urban area and finally reaches another suburban area or crosses another urban area. In this study, this line is called the UHI line. The UHI phenomenon represents the higher atmospheric temperature and LST in the urban area than in the suburban area, which can be used to detect the urbanization rate (Grover and Singh, 2015; Yuan and Bauer, 2007). The increase of UHI is affected by anthropogenic heat generated from traffic, LULC change, and increase of impervious area, and it affects the urban climate because of the exchange of energy and level of conductivity (Alexander, 2020; Neinavaz *et al.,* 2020; Sekertekin and Bonafoni, 2020). The change of LST is closely related to the change of UHI because UHI is part of the LST located at the center of an urbanized area. The values of NDVI, NDBI, and LST along the UHI line will be used as data to analyze their relationship with each other. LST and NDVI have a reverse relationship, i.e., the decrease of NDVI will affect the increase of LST (Arnon *et al.,* 2010; Guha *et al.,* 2018; Hua and Ping, 2018). The increase of LST will affect the change of the local climate, including the change in the rainfall characteristics.

Rainfall characteristics

The rainfall characteristics can be indicated by the maximum, minimum, and average values of rainfall intensity and the NRD in a certain period. The rainfall data are recorded by rainfall stations that are located around an area. Each rainfall station has an influence area. Several methods are employed to analyze the influence area of the rainfall station. One method that is commonly used in hydrologic analysis is the Thiessen polygon method (Brassel and Reif, 2010; Fiedler, 2003). The influence area of the rainfall station is obtained by drawing perpendicular bisectors on lines intersecting near the stations to form a series of polygons, each containing one and only one rainfall station, and leaving the other stations at the center of the polygons, which will vary in size according to the spacing of the stations. Based on the Thiessen polygon of each research area, the LST image of each research area is cropped. The relationship between

the changes of LST in the influence area of each rainfall station and the changes of the maximum, minimum, and average values of rainfall intensity and NRD of each research area will be investigated.

RESULTS AND DISCUSSION

The imagery data used in this study are Landsat 5 TM, Landsat 7 ETM+, and Landsat 8 OLI scanned in 1995, 2001, 2015, and 2020. All of the imagery data were downloaded from the USGS through the USGS Earth Explorer. In the study area, no cloud cover percentage <10% was observed. As a result, 5-year interval imagery data starting in 1995 cannot be obtained. The imageries scanned in 2000 were significantly different from the imageries scanned in 2001. Due to the percentage of cloud cover, the best imageries of ETM+ covering the Probolinggo Regency, Sampang Regency, and Surabaya City was obtained in 2002. The overall imageries used in this study are shown in Table 2. The ArcGIS software was used to analyze the Landsat imagery data.

From Table 2 it can be seen that the satellite images used were scanned between May to August or during dry season in Indonesia. In this season, there are relatively low cloud cover so that a relatively clean images can be obtained. In the result, all images with cloud cover less than 10% can be obtained for this study. The rainfall data were obtained from the East Java Province Water Resources Agency (Dinas Pengairan Provinsi Jawa Timur). The number of rainfall stations used in this study depends on the availability of stations for each research area. Based on the availability of data, the daily rainfall data are used in this study. The maximum, minimum, and average values of rainfall intensity and the NRD data in the same year as the satellite imagery data are used in this study.

Relationship between NDVI and LST

The NDVI of all research areas was calculated using Eqs. 1 or 2. By using these Eqs., the minimum and maximum values of the NDVI of all research areas was analyzed. The result is shown that the negative NDVI decreases year by year, whereas the positive NDVI remains the same year by year. This finding indicates that some areas covered by vegetation were converted into areas covered by manmade materials, built-up areas, or bare land. For example, the 1995 and 2020 NDVI of Malang and Surabaya cities is shown in Fig. 3. This figure shows that the greenness displayed in green colour decreased from 1995 to 2020 to the non-greenness area displayed in brown colour.

If the NDVI in the study area decreases, then solar energy will be reflected and emitted by manmade materials. The manmade materials strongly reflected the solar energy, then the LST will increase. To determine the relationship between NDVI and LST, the LST of the research area needs to be analyzed using Eqs. 4 to 11. For the Landsat 5 TM and Landsat 7 ETM+ imageries, $QCAL_{max}$ is equal to 255 and $QCAL_{min}$ is equal to 1. For Band 6, $L_{max\lambda}$ is equal to 15.303 and

Table 2: Landsat imagery data.

No.	Path/row	Sensor	Acquisition date	Location
1.	118/066	L5-TM	May 24, 1995	Malang Regency Malang City Batu City
2.	118/065	L5-TM	June 25, 1995	Probolinggo Regency Surabaya City
3.	118/065	L5-TM	July 27, 1995	Sampang Regency
4.	119/065	L5-TM	August 03, 1995	Tuban Regency
5.	118/066	L7-ETM	August 04, 2001	Malang Regency Malang City Batu City
6	118/065	L7-ETM	August 23, 2002	Probolinggo Regency Sampang Regency
7	118/065	L7-ETM	May 19, 2002	Surabaya City
8	119/065	L7-ETM	August 27, 2001	Tuban Regency
9	118/066	L8-OLI	June 16, 2015	Malang Regency Malang City Batu City
10	118/065	L8-OLI	June 16, 2015	Probolinggo Regency Surabaya City Sampang Regency
11	119/065	L8-OLI	June 23, 2015	Tuban Regency
12	118/066	L8-OLI	June 13, 2020	Malang Regency Malang City Batu City Probolinggo Regency
13	118/065	L8-OLI	July 31, 2020	Sampang Regency
14	118/065	L8-OLI	June 13, 2020	Surabaya City
15	119/065	L8-OLI	August 23, 2020	Tuban Regency

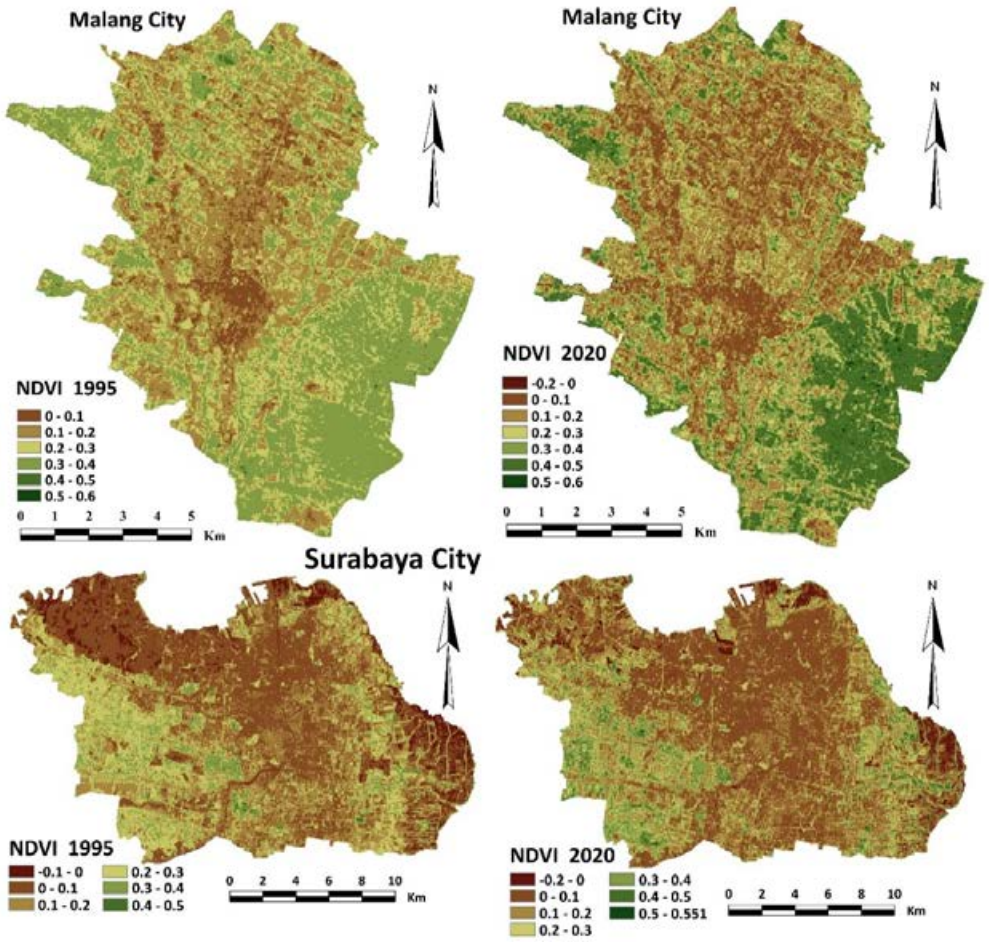

Fig. 3: NDVI of Malang and Surabaya cities in 1995 and 2020

$L_{min\lambda}$ is equal to 1.23. The other parameters used to analyze LST from the Landsat 5 TM and Landsat 7 ETM+ imageries are K_1 and K_2. Here, K_1 is equal to 607.76 and 666.09, and K_2 is equal to 1,260.56 and 1,282.71 for Landsat 5 TM and Landsat 7 ETM+ imageries, respectively. For Landsat 8 OLI, K_1 and K_2 for Band 10 are equal to 774.89 and 1,321.08, respectively. From the MTL file on the Landsat 8 OLI data used in this study, the M_L and A_L values for Band 10 are equal to 0.0003342 and 0.1, respectively. Based on these parameters and the corresponding DN of satellite imagery data, the LST of all research areas was analyzed. The summary of the LST analysis results shows that the maximum and minimum values of LST in all research areas increase year by year from 1995 to 2020. The maximum LST in Surabaya City and Tuban Regency increased. For Surabaya City, the maximum LST increased from 28°C in 1995 to 34°C in 2020, i.e., up to 6°C. This finding indicates that Surabaya City is undergoing rapid urbanization because it is the second largest city in Indonesia. For Tuban Regency, the maximum LST increased from 28°C in 1995 to 37.2°C in 2020, i.e., up to 9.2°C. This finding indicates that Tuban Regency is one of the areas in East Java Province that has many oil mining areas with high demand for oil fuel energy (BPS-STR, 2021). The LST changes from 1995 to 2020 and the LST

imageries of Surabaya City and Tuban Regency are shown in Fig. 4. It is shown that the dark red colour increased from 1995 to 2020, meaning the LST trend increased. The NDVI tends to decrease year by year,

whereas the LST tends to increase year by year. To obtain a clear understanding of these phenomena, the relationship between NDVI and LST needs to be analyzed. To simplify the analysis of this relationship, the picture element (pixel) of the NDVI and LST of each research area generated from the UHI will be compared. The UHI is the occurrence of LST in urbanized areas compared with the LST in suburban areas. In this study, the UHI is represented by a line drawn from a suburban area to a central urban area and another suburban area. In this study, this line is called the UHI line. The pixel values of the NDVI and LST along the UHI line will be compared to determine the relationship between NDVI and LST in all research areas. For example, the UHI line of Probolinggo Regency drawn on the land cover imageries is shown in Fig. 5. The maximum and minimum values of NDVI and LST along the UHI line of all research areas are summarized in Tables 3 and 4. Table 3 shows that the minimum value of NDVI in 2001 is negative, which indicates that some pixels along the UHI line are not covered by vegetation. The minimum values of NDVI in the other years are all positive, which indicates that some pixels along the UHI line are covered by vegetation. This phenomenon indicates that, after the reformation era (i.e., 1998), deforestation in East Java Province occurred poorly. Tabel 4 shows that the LST almost increase year by year. A decrease in NDVI causes the energy of sunlight to be reflected and emitted strongly and causes the LST to rise. The relationship between NDVI and LST was depicted in graphs. The trend line was drawn, and regression analysis was conducted. Each research area has four graphs for 1995,

2001, 2015, and 2020. Therefore, a total of 28 graphs are generated for the relationship between NDVI and LST in the entire research area. Six of the 28 graphs are shown in Fig. 6 as examples. The summary of 24 regression analyses, which consist of regression equations and coefficients of determination, is shown

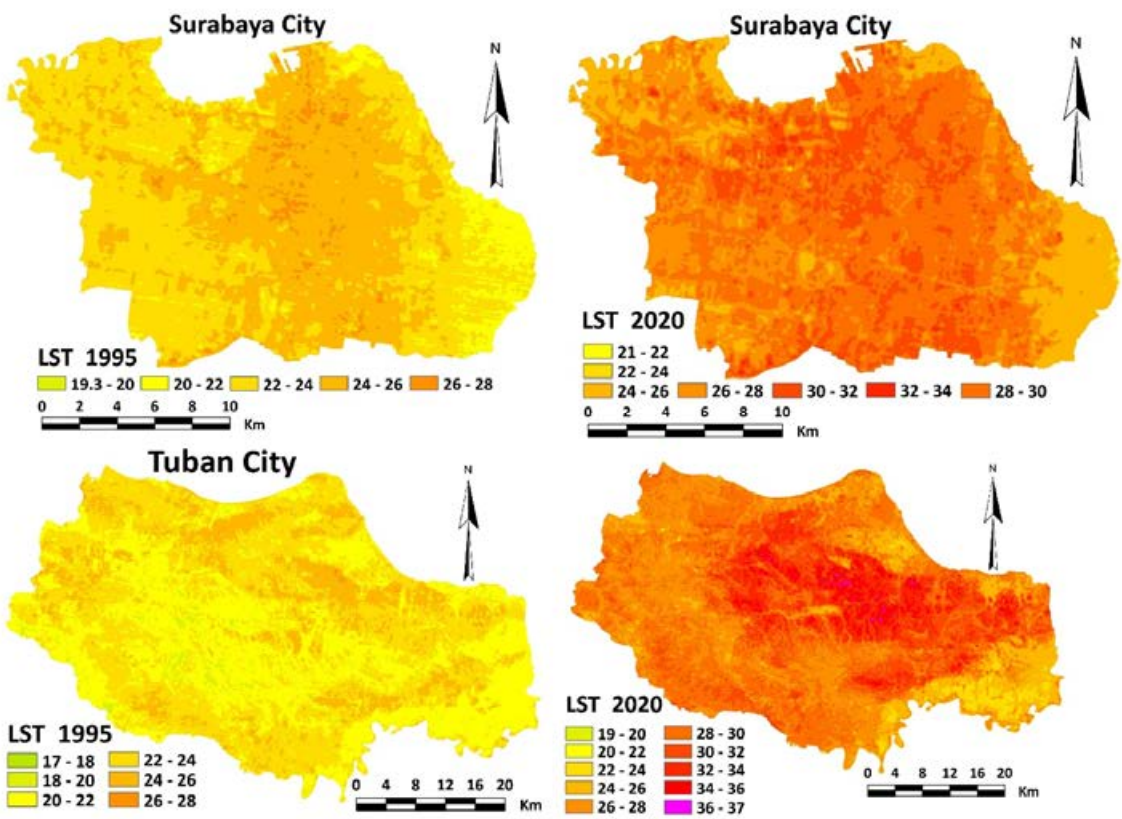

Fig. 4: LST of Surabaya City and Tuban Regency in 1995 and 2020

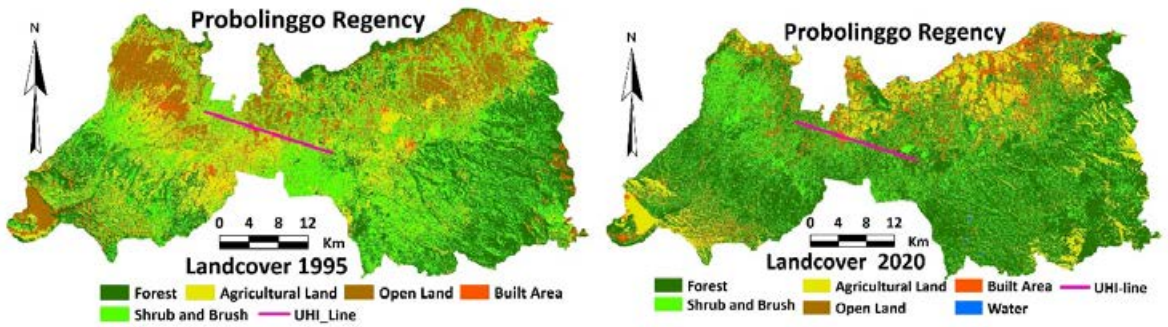

Fig. 5: UHI line of probolinggo regency

Table 3: NDVI along the UHI lines

Research areas	NDVI							
	1995		2001		2015		2020	
	Min.	Max.	Min.	Max.	Min.	Max.	Min.	Max.
Batu City	0.1	0.4	−0.2	0.4	0.0	0.4	0.0	0.5
Malang City	0.0	0.4	−0.3	0.4	0.0	0.5	0.0	0.5
Surabaya City	0.0	0.4	−0.6	0.4	0.0	0.5	0.0	0.5
Malang Regency	0.1	0.4	−0.3	0.5	0.1	0.5	0.1	0.5
Probolinggo Regency	0.1	0.4	−0.3	0.3	0.1	0.5	0.1	0.5
Sampang Regency	0.1	0.4	−0.3	0.3	0.0	0.5	0.0	0.5
Tuban Regency	0.1	0.4	−0.4	0.3	−0.1	0.5	0.0	0.5

Table 4: LST along the UHI lines

Research areas	LST (°C)							
	1995		2001		2015		2020	
	Min.	Max.	Min.	Max.	Min.	Max.	Min.	Max.
Batu City	17.5	26.6	22.1	36.2	20.6	28.0	21.5	28.5
Malang City	19.3	27.5	25.6	35.1	22.7	30.8	22.7	30.0
Surabaya City	20.2	26.7	20.4	33.4	23.5	30.4	22.2	31.4
Malang Regency	19.2	26.2	23.1	32.6	21.1	29.6	22.1	29.7
Probolinggo Regency	22.0	25.4	26.6	33.2	16.9	26.7	23.0	29.7
Sampang Regency	21.9	25.4	24.6	32.5	19.0	29.2	21.7	28.0
Tuban Regency	19.7	25.0	27.8	37.4	23.4	32.9	24.2	36.5

in Table 5. This table shows that all coefficients of regression have a negative value, indicating that NDVI is inversely proportional to LST and this inline with Alexander (2020) and Garouani *et al.* (2021) research results. If the NDVI decreases, then the LST increases and if the percentage of land covered by vegetation decreases, then the LST increases because the area that absorbs the emitted solar energy decreases. This table also shows that nearly all coefficients of determination (or R^2) are >0.5. This finding indicates that the relationship between NDVI and LST is nearly inversely proportional. For Surabaya City, the R^2 values in 1995, 2001, and 2015 are <0.1. This finding indicates that, in Surabaya City, many objects have a small NDVI and do not affect the LST, particularly the objects along the UHI line, such as barren soil, open land, and water.

Relationship between NDVI and NDBI

The built-up area is indicated by the changes of natural land cover to artificial land cover, such as housing, asphalt, concrete, and parking lot. The built-up area can be well detected using Landsat imagery data (Bhatti and Tripathi, 2014). In this study, NDBI was used to analyze the proportion of built-up area and calculated using Eq. 3. The calculated results of

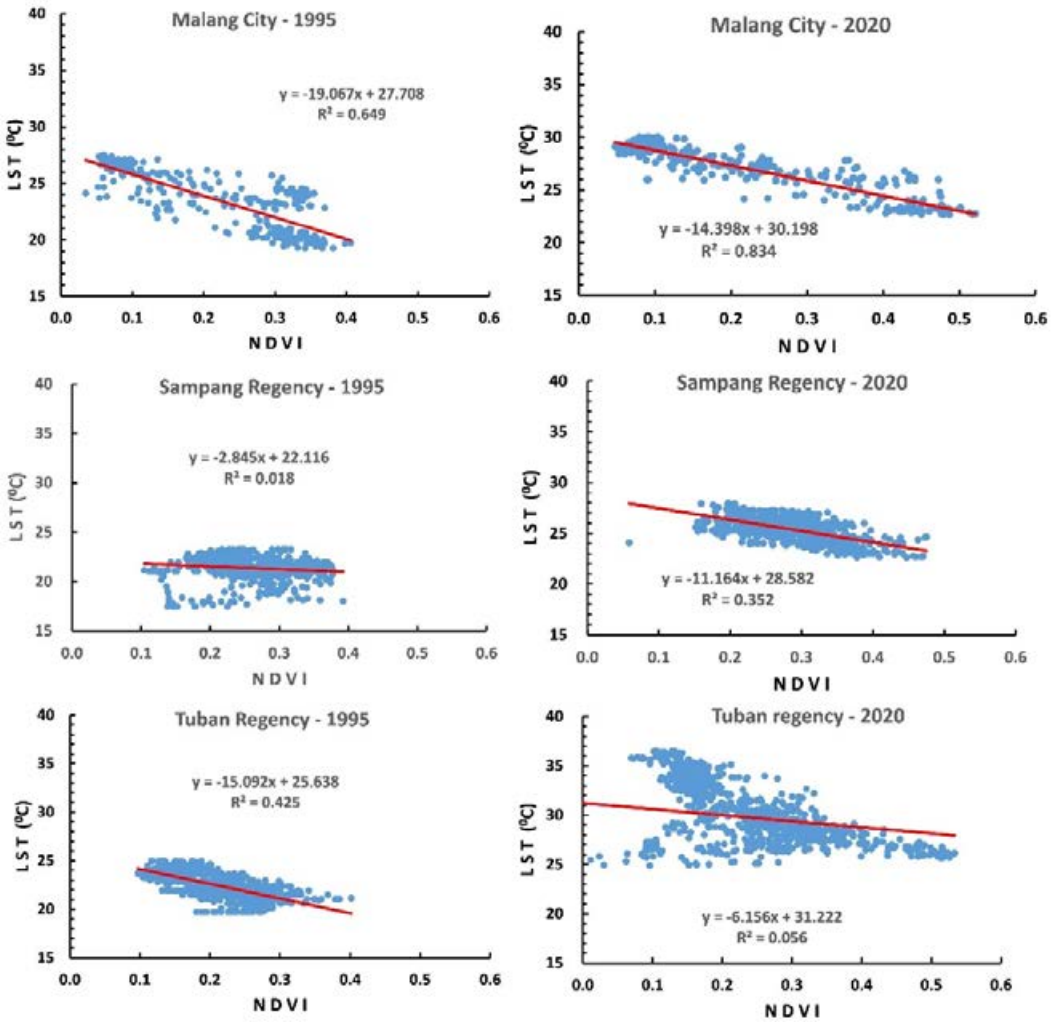

Fig. 6: Relationship between NDVI and LST

NDBI represented by the minimum and maximum values of the entire research area are shown in Table 6. The maximum values of the NDBI of three cities in the research area, i.e., Batu, Malang, and Surabaya, are higher than those of three regencies in the study area, i.e., Probolinggo, Sampang, and Tuban. The maximum value of the NDBI of Malang Regency is higher than those of the three other regencies because Malang Regency is categorized as a developed regency in East Java Province (BPS-SMR, 2021). As mentioned previously, the NDBI indicates the proportion of built-up area, whereas the NDVI indicates the proportion of land covered by vegetation. Urbanization is the change of land covered by vegetation to land covered by manmade materials, such as houses, concrete, and asphalt. Urbanization will extend the built-up area to meet the need for housing, offices, business areas, and accessibility due to population growth. Development of these infrastructures will occupy the land covered by vegetation. The land covered by vegetation will decrease and the land covered by built-up area will be increased. The relationship between NDVI and NDVI should be inversely proportional.

To compare it, the NDBI along the UHI line of each research area needs to be calculated. The calculated results represented by the minimum and maximum values of each research area from 1995 to 2020 are

Table 5: Relationship between NDVI and LST

Research areas	Years	Regression Eq.	Regression coefficient
Batu City	1995	$y = -18.377x + 28.261$	0.489
	2001	$y = -16.583x + 31.938$	0.651
	2015	$y = -13.927x + 29.027$	0.502
	2020	$y = -11.822x + 28.808$	0.479
Malang City	1995	$y = -19.067x + 27.708$	0.649
	2001	$y = -12.218x + 30.492$	0.855
	2015	$y = -15.758x + 30.241$	0.827
	2020	$y = -14.398x + 30.198$	0.834
Surabaya City	1995	$y = -2.714x + 24.301$	0.028
	2001	$y = -2.769x + 28.57$	0.030
	2015	$y = -5.756x + 28.351$	0.092
	2020	$y = -8.421x + 29.647$	0.227
Malang Regency	1995	$y = -4.852x + 23.417$	0.115
	2001	$y = -7.106x + 28.139$	0.413
	2015	$y = -7.093x + 25.954$	0.287
	2020	$y = -9.667x + 27.946$	0.479
Probolinggo Regency	1995	$y = -6.064x + 24.827$	0.342
	2001	$y = -11.581x + 29.773$	0.579
	2015	$y = -20.187x + 28.83$	0.423
	2020	$y = -11.27x + 29.984$	0.600
Sampang Regency	1995	$y = -2.845x + 22.116$	0.018
	2001	$y = -8.294x + 29.74$	0.501
	2015	$y = -6.992x + 28.067$	0.085
	2020	$y = -11.164x + 28.582$	0.352
Tuban Regency	1995	$y = -15.092x + 2.638$	0.425
	2001	$y = -12.681x + 31.462$	0.404
	2015	$y = -10.392x + 30.351$	0.187
	2020	$y = -6.156x + 31.222$	0.056

Table 6: NDBI of the research areas

Research areas	NDBI							
	1995		2001		2015		2020	
	Min.	Max.	Min.	Max.	Min.	Max.	Min.	Max.
Batu City	−0.47	0.41	−0.37	0.48	−0.48	0.26	−0.47	0.25
Malang City	−0.36	0.47	−0.40	0.60	−0.34	0.27	−0.35	0.31
Surabaya City	−0.36	0.45	−0.58	0.58	−0.41	0.30	−0.41	0.36
Malang Regency	−0.65	0.55	−0.56	0.62	−0.45	0.48	−0.46	0.50
Probolinggo Regency	−0.40	0.40	−0.51	0.65	−0.47	0.26	−0.48	0.30
Sampang Regency	−0.41	0.28	−0.70	0.6	−0.48	0.21	−0.47	0.24
Tuban Regency	−0.32	0.25	−0.36	0.58	−0.42	0.60	−0.43	0.41

shown in Table 7. Compared with the minimum value of NDBI of each research area, the minimum value of NDBI along the UHI line is lower because the UHI line is initially drawn from a suburban area to an urban area and finally reaches another suburban area. By drawing a two-dimensional graph of NDVI and NDBI, the relationship between both factors can be represented. Based on the number of research areas and the number of years, a total of 28 NDVI–NDBI graphs are generated. Six of the 28 graphs are shown in Fig. 7 as examples. This figure shows that NDVI is inversely proportional to NDBI. The regression equations of the relationship between NDVI and NDBI for all research areas are shown that all of the coefficients of regression are negative, with more than 50% having values less than −0.7. The results show that 2 areas have coefficients of regression greater than −0.5, 3 areas have coefficients of regression between −0.5 and −0.7, 17 areas have coefficients of regression between −0.7 and −1, and 2 areas have coefficients of regression less than −1. The coefficients of determination of nearly all areas

Table 7: NDBI along the UHI lines

Research areas	NDBI							
	1995		2001		2015		2020	
	Min.	Max.	Min.	Max.	Min.	Max.	Min.	Max.
Batu City	−0.30	0.26	−0.16	0.31	−0.29	0.08	−0.29	0.13
Malang City	−0.36	0.47	−0.10	0.37	−0.31	0.09	−0.34	0.11
Surabaya City	−0.23	0.12	−0.23	0.47	−0.33	0.13	−0.32	0.17
Malang Regency	−0.28	0.27	−0.19	0.34	−0.34	0.09	−0.32	0.10
Probolinggo Regency	−0.23	0.05	−0.09	0.34	−0.31	0.06	−0.36	0.14
Sampang Regency	−0.24	0.06	−0.31	0.37	−0.23	0.05	−0.24	0.10
Tuban Regency	−0.20	0.08	−0.13	0.14	−0.29	0.11	−0.33	0.11

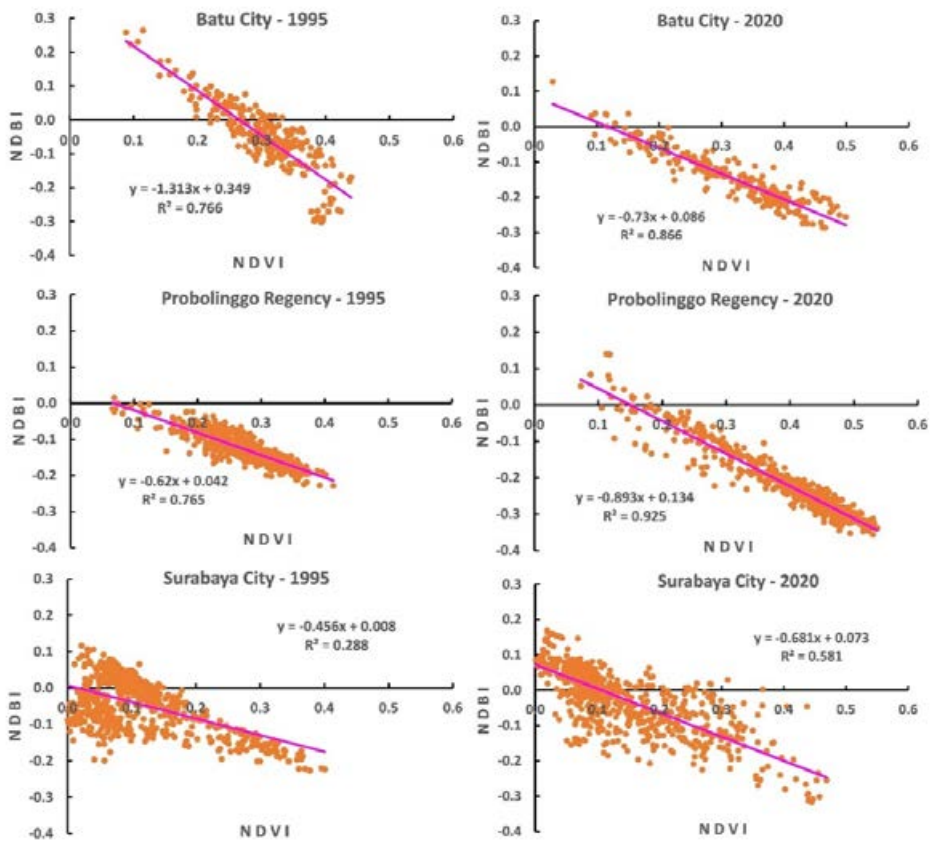

Fig. 7: Relationship between NDVI and NDBI

are >0.5, and only two areas have values <0.5. This finding indicates that NDVI is significantly inversely proportional to NDBI. This result show a clearer relationship quantitatively than the results of Grover and Singh (2015) and Guha *et al.* (2018)'s research. In the same manner, the relationship between NDBI and LST was analyzed.

Fig. 8 shows the graph of the relationship between NDBI and LST in six research areas as an example. The regression analysis results of the relationship between NDBI and LST of the entire research area are shown in Table 8. Table 8 show that NDBI is directly proportional to LST, with a significant coefficient of regression. Among the 28 research areas, 14 areas have a coefficient of determination (R^2) >0.5 and the minimum R^2 is equal to 4.194. This correlation

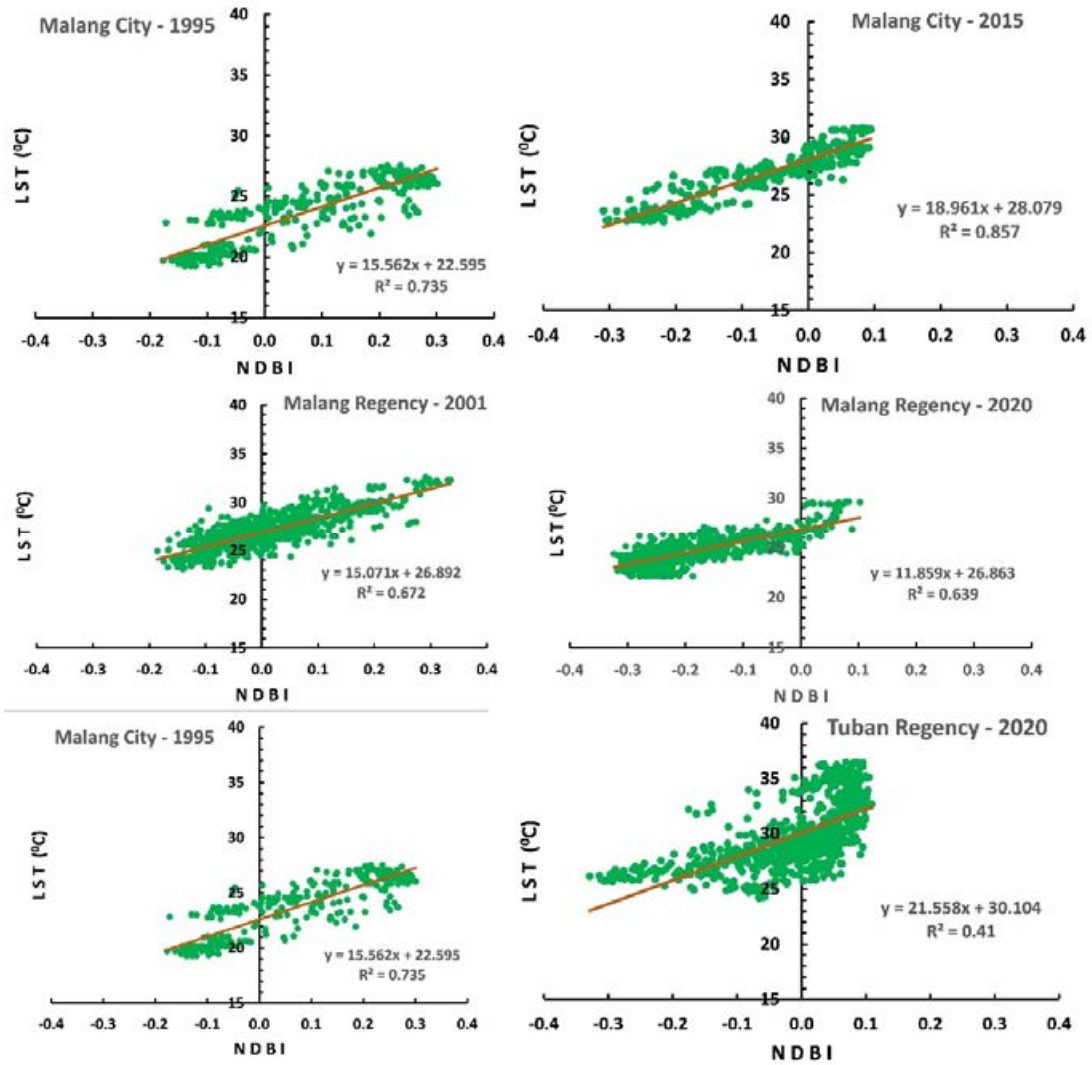

Fig. 8: Relationship between NDBI and LST.

was observed at Surabaya City in 2001, where the development was not yet fully underway. These results show that the relationship between NDBI and LST is clearer than the results of Ibrahim (2017)'s study which was only conducted in one location. Research conducted by Ranagalage *et al.* (2017) resulted in the relationship between urbanization and LST.

Rainfall characteristics

The increase of LST will affect the rainfall characteristics. The relationship between convective precipitation frequency and LST is insignificant (Shiraki and Shigeta, 2013). Meanwhile, Himayoun *et al.* (2020) stated that the increase of LST will intensify precipitation. To verify their statement and to find out the relationship between the two parameters more clearly, the relationship between LST and rainfall characteristics is investigated. The NRD and the average and maximum values of rainfall intensity are considered the rainfall characteristics in this research. The analysis of the relationship between LST and rainfall characteristics was done by comparing the

LST and rainfall characteristics

in each area of the Thiessen polygon for each year. The area of the Thiessen polygon of each

Table 8: Relationship between NDBI and LST

Research areas	Years	Regression Eq.	R^2
Batu City	1995	$y = 14.429x + 23.298$	0.679
	2001	$y = 27.752x + 27.343$	0.762
	2015	$y = 18.285x + 27.306$	0.596
	2020	$y = 16.716x + 27.495$	0.589
Malang City	1995	$y = 15.562x + 22.595$	0.735
	2001	$y = 18.775x + 27.543$	0.823
	2015	$y = 18.961x + 28.079$	0.857
	2020	$y = 16.492x + 27.988$	0.826
Surabaya City	1995	$y = 14.802x + 24.627$	0.601
	2001	$y = 4.194x + 27.143$	0.280
	2015	$y = 11.139x + 28.063$	0.396
	2020	$y = 10.137x + 28.702$	0.263
Malang Regency	1995	$y = 6.825x + 22.739$	0.326
	2001	$y = 15.071x + 26.892$	0.673
	2015	$y = 13.048x + 26.066$	0.548
	2020	$y = 11.859x + 26.863$	0.639
Probolinggo Regency	1995	$y = 10.265x + 24.473$	0.492
	2001	$y = 14.083x + 28.670$	0.417
	2015	$y = 23.852x + 26.646$	0.474
	2020	$y = 11.898x + 28.135$	0.576
Sampang Regency	1995	$y = 9.598x + 21.852$	0.109
	2001	$y = 11.259x + 27.686$	0.777
	2015	$y = 15.651x + 27.336$	0.313
	2020	$y = 10.722x + 25.886$	0.270
Tuban Regency	1995	$y = 15.317x + 22.754$	0.374
	2001	$y = 28.498x + 31.707$	0.365
	2015	$y = 20.631x + 28.799$	0.496
	2020	$y = 21.558x + 30.104$	0.410

research area was drawn based on the number of rainfall stations in each research area. For example, the Probolinggo Regency has 11 rainfall stations. The Thiessen polygon can be drawn based on the locations of the rainfall stations, and the result is shown in Fig. 9. The daily rainfall data are used in this study. The rainfall characteristics of each rainfall station are represented by the average and maximum daily rainfall per year. The rainfall characteristics of Probolinggo Regency from 1995 to 2020 are shown in Table 9.

In case of Probolinggo Regency, the average rainfall intensity during 2015 is higher than 2020, but the maximum rainfall intensity is lower. Due to the Lanina effect, this phenomenon occurs because the rain that occurred in 2020 was not evenly distributed throughout the region like the rain that occurred in 2020. But the maximum rainfall intensity in 2020, will still be higher than in 2015. Based on the Thiessen polygon of Probolinggo Regency, the LST image was cropped, and the average and maximum LST of each area of the Thiessen polygon were calculated. The rainfall characteristics of each rainfall station and the average of maximum LST of each research area in 1995, 2001, 2015, and 2020 of Probolinggo Regency were analyzed based on the Thiessen polygon. The analyses of other research areas were conducted in the same manner. The relationship between LST and rainfall characteristics, especially the average of maximum rainfall intensity and NRD was analyzed. The graph of the relationship between average LST and average of maximum rainfall intensity is shown in Fig. 10. This figure shows that LST is directly proportional to rainfall intensity. However, the coefficient of regression is only equal to 0.1. This finding indicates that the correlation between LST and rainfall intensity is weak but directly proportional. Thus, the increase of LST has a weak relationship with the increase of rainfall intensity. Similarly, the graph of the relationship between LST and NRD is shown in Fig. 10. The graph illustrates that LST has an inverse relationship with NRD or NRD per year. The coefficient of regression is −1.89, and the coefficient of correlation is 0.1. This finding indicates

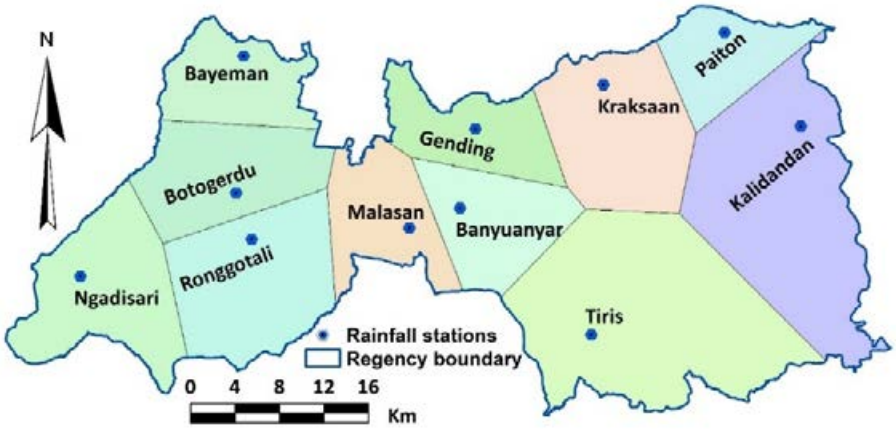

Fig. 9: Thiessen polygon of probolinggo regency

Table 9: Rainfall characteristics of probolinggo regency

No.	Rainfall stations	Rainfall intensity (mm/day)							
		1995		2001		2015		2020	
		Ave.	Max.	Ave.	Max.	Ave.	Max.	Ave.	Max.
1.	Banyuanyar	20.6	95	24.6	92	35.6	110	22.3	135
2.	Bayeman	22.8	121	11.6	54	23.5	120	17.1	109
3.	Botogerdu	22.5	80	24.8	84	35.7	97	25.6	95
4.	Gending	24.3	95	15.3	75	28.9	98	21.6	201
5.	Kalidandan	25.3	92	21.7	89	31.2	148	17.7	110
6.	Kraksaan	24.5	106	30.3	145	19.6	102	22.7	168
7.	Malasan	23.7	102	21.6	87	22.6	165	29.5	215
8.	Ngadisari	17.4	99	24.7	332	14.7	55	17.4	49
9.	Paiton	32.3	188	24.8	158	27.5	89	32.6	140
10.	Ronggotali	20.6	125	23.3	84	30.2	173	33.7	120
11.	Tiris	25.7	80	25.9	87	23.5	164	26.3	185

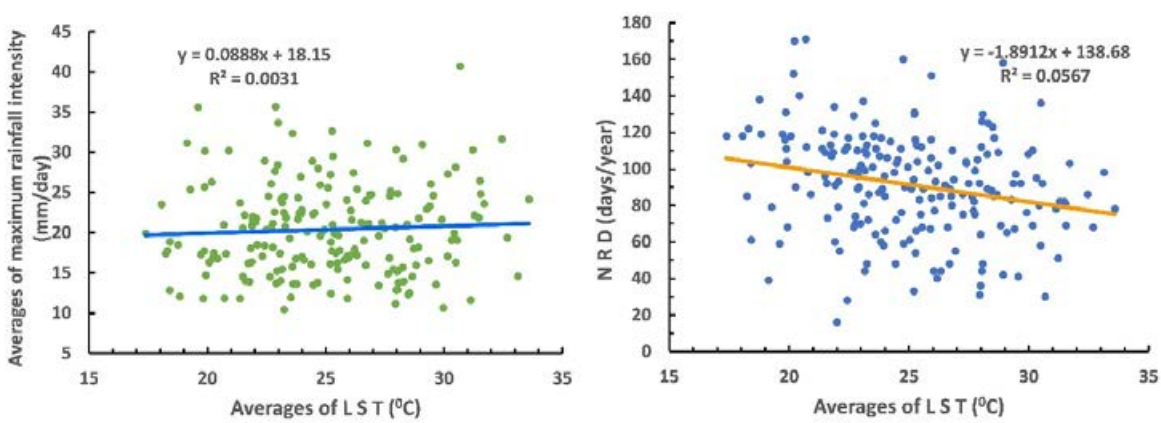

Fig. 10: Relationship between LST and rainfall intensity and LST–NRD

that the correlation between LST and NRD is low with an inverse relationship. Quantitatively, this result is clearer than the research conducted by Garouani *et al.* (2021), Himayoun *et al.* (2020), Hu *et al.* (2020), and Shiraki and Shigeta (2013). The resulting regression equations can be used to estimate the increase in rainfall intensity and decrease in NRD in East Java Province Indonesia caused by decreasing in environmental conditions that cause an increase in LST.

CONCLUSION

In this research, Landsat TM, ETM+, and OLI were used to identify the relationship between NDVI and LST, between NDVI and NDBI, between NDBI and LST, and between LST and rainfall characteristics. Seven areas in East Java Province were used as test areas. The pixel values of NDVI, NDBI, and LST along the UHI line were used to analyze the relationship between NDVI and LST, between NDVI and NDBI, and between NDBI and LST. The UHI line is initially drawn from a suburban area to an urban area and finally reaches another suburban area. Meanwhile, the pixel values generated from the area of the Thiessen polygon were used to analyze the relationship between LST and rainfall characteristics. The analysis results show that NDVI is significantly inversely proportional to LST. All of the coefficients of regression have negative values, and the coefficients of determination (R^2) have values >0.4 in 16 of the 24 research areas. The analysis results of the relationship between NDVI and NDBI show that NDVI is significantly inversely proportional to NDBI. The regression equation for each research area shows that all of the coefficients of regression are negative, with more than 50% having values less than −0.7, and the coefficients of determination are approximately >0.5. This relationship is plausible because NDVI indicates land covered by vegetation and NDBI indicates land covered by manmade materials or built-up areas. The relationship between NDBI and LST was analyzed in the same manner as the relationship between NDVI and LST. The analysis results show that NDBI is significantly directly proportional to LST. The regression equations of all areas show that 14 areas have the minimum coefficient of regression, i.e., equal to 4.194, with R^2 values >0.5. Thus, the increase of the built-up area influences the increase of LST. Finally, the relationship between LST and rainfall characteristics was investigated. The analysis results show that LST has a fairly weak but directly proportional relationship with rainfall intensity, as indicated by the coefficients of regression and determination, both of which are <0.1. Meanwhile, the relationship between LST and the NRD has an inverse relationship, which is also fairly weak, as indicated by a coefficient of regression that is equal to −1.891 and an R^2 that is <0.1. This research shows that LULC change indicated by NDVI and NDBI changes will significantly affect LST. The change of LST will have a fairly weak effect on rainfall intensity and NRD.

AUTHOR CONTRIBUTIONS

A. Suharyanto, the corresponding author has contributed to supervising the fourth and fifth authors in the data analysis NDVI and rainfall analysis, interpreting the results, and preparing the manuscript. A. Maulana helped in the LST and NDBI data analyses. D. Suprayogo designed the analysis of NDVI and LST. Y.P. Devia prepared all the tables and figures and interpretation of the results, especially in NDVI. S. Kurniawan prepared all the maps and interpretation of the relation with rainfall data.

ACKNOWLEDGEMENT

The research was conducted in three cities and four regencies in East Java Province Indonesia by the research team from Universitas Brawijaya and Universitas Hasanuddin. This research is partially funded by the Indonesian Ministry of Research and Technology/National Agency for Research and Innovation and the Indonesian Ministry of Education and Culture under the World-Class University (WCU) Program managed by Institut Teknologi Bandung with grant number [1920B/I1.B04.2/SPP/2020] and Doktor Lektor Kepala research grant Faculty of Engineering Universitas Brawijaya with number [17/UN10.F07/PN/2022]. The authors also thank Dinas Pengairan Provinsi Jawa Timur, Balai Besar Wilayah Sungai Brantas for providing the rainfall data. Finally, the authors are indebted to the USGS. The proofreading of the manuscript is supported by Enago.

CONFLICT OF INTEREST

The author declares that there is no conflict of interests regarding the publication of this manuscript. In addition, the ethical issues, including plagiarism, informed consent, misconduct, data fabrication and/

or falsification, double publication and/or submission, and redundancy have been completely observed by the authors.

OPEN ACCESS

PUBLISHER'S NOTE

ABBREVIATIONS

%	Percent
µm	Micrometer
AL	Specific additive rescaling factor
BPS	Badan pusat statistik (Central bureau of statistics)
C	Celsius
DN	Digital number
E	Error correction
Eq.	Equation
ETM+	Enhanced Thematic Mapper+
GIS	Geographic Information System
i.e.	Id est (that is)
J	Joule
K_1	Specific thermal conversion constant 1
K_2	Specific thermal conversion constant 2
K	Kelvin
Km	Kilometer
L5	Landsat 5
L7	Landsat 7
L8	Landsat 8
LST	Land surface temperature
LULC	Land use/land cover
m	Meter
max.	Maximum
min	Minimum
M_L	Specific multiplicative rescaling factor
MTL	Metadata text file extension
NDBI	Normalized Difference Built-up Index
NDVI	Normalized Difference Vegetation Index
N	North
NIR	Near-infrared
NRD	Number of rainfall days
OLI	Operational Land Imager
PV	Proportional vegetation
Q_{cal}	Quantized and calibrated standard product pixel values
s	Second
SWIR	Sort wave infrared
T	Temperature
TC	Temperature Celsius
TIRS	Thermal infrared sensor or Thermal infrared scanner
TM	Thematic Mapper
TOA	Top of atmospheric
UHI	Urban heat island
USGS	United State Geological Survey

REFERENCES

Alexander, C., (2020). Normalised difference spectral indices and urban land cover as indicators of land surface temperature (LST). Int. J. Appl. Earth Obs. Geoinf., 86: 102013 **(11 pages)**.

Almeida, C.R.; Teodoro, A.C.; Gonçalves, A., (2021). Study of the urban heat island (UHI) using remote sensing data/techniques: A systematic review. Environment, 8(10): 105 **(39 pages)**.

Almouctar, M.A.S.; Wu, Y.; Kumar, A.; Zhao, F.; Mambu, K.J.; Sadek, M., (2021). Spatiotemporal analysis of vegetation cover changes around surface water based on NDVI: A case study in Korama basin, Southern Zinder, Niger. Appl. Water Sci., 11(4): 1-14 **(14 pages)**.

Anache, J. A.A.; Wendland, E.C.; Oliveira, P.T.S.; Flanagan, D.C.; Nearing, M.A., (2017). Runoff and soil erosion plot-scale studies under natural rainfall: A meta-analysis of the Brazilian experience. CATENA, 152: 29-39 **(11 pages)**.

Arnon, K.; Agam, N.; Pinker, R.T.; Anderson, M.; Imhoff, M.L.; Gutman, G.G.; Panov, N.; Goldberg, A., (2010). Use of NDVI and land surface temperature for drought assessment: Merit and limitations. J. Clim., 23: 618-633 **(16 pages)**.

Badlani, B.; Patel, A.N.; Patel, K.; Kalubarme, M.H., (2017). Urban growth monitoring using remote sensing and geo-informatics: case study of Gandhinagar, Gujarat State (India). Int. J. Geosciences, 08(4): 563-576 **(14 pages)**.

Bhatti, S.S.; Tripathi, N.K., (2014). Built-up area extraction using Landsat 8 OLI imagery. GISci. Remote Sens., 51(4): 445-467 **(23 pages)**.

Bonafoni, S.; Anniballe, R.; Gioli, B.; Toscano, P., (2016). Downscaling Landsat land surface temperature over the urban area of Florence. Eur. J. Remote Sens., 49(1): 553-569 **(17 pages)**.

BPS-SJTP, (2021). Jawa Timur Province in figures.

BPS-SMR, (2021). Malang Regency in figures.

BPS-SSM, (2021). Surabaya Municipality in figures.

BPS-STR, (2021). Tuban Regency in figures.

Brassel, K.E.; Reif, D., (2010). A procedure to generate Thiessen polygons. Geog. Anal., 11(3): 289-303 **(15 pages)**.

Chang, M.E.; Zhao, Z.Q.; Chang, H.T.; Shu, B., (2021). Urban green infrastructure health assessment, based on Landsat 8 remote sensing and entropy landscape metrics. Eur. J. Remote Sens., 54(1): 417-430 (**14 pages**).

Chen, P.; Liu, H.; Wang, Z.; Mao, D.; Liang, C.; Wen, L.; Li, Z.; Zhang, J.; Liu, D.; Zhuo, Y.; Wang, L., (2021). Vegetation dynamic assessment by NDVI and field observations for sustainability of China's Wulagai river basin. Int. J. Environ. Res. Public Health, 18(5): **(20 pages)**.

Derdouri, A.; Wang, R.; Murayama, Y.; Osaragi, T., (2021). Understanding the links between LULC changes and SUHI in cities: Insights from two-decadal studies (2001-2020). Remote Sens., 13(18): 3654 **(34 pages)**.

Devi, R.M.; Prasetya, T.A.E.; Indriani, D., (2020). Spatial and temporal analysis of land surface temperature change on New Britain Island. Int. J. Remote Sens. Earth Sci., 17(1): **(12 pages)**.

Ferrelli, F.; Cisneros, M.A.H.; Delgado, A.L.; Piccolo, M.C., (2018). Spatial and temporal analysis of the LST-NDVI relationship for the study of land cover changes and their contribution to urban planning in Monte Hermoso, Argentina. Documents d'Analisi Geografica, 64(1).

Fiedler, F.R., (2003). Simple, Practical method for determining station weights using Thiessen polygons and Isohyetal maps. J. Hydrol. Eng., 8(4): 219.

Firozjaei, M.K.; Sedighi, A.; Kiavarz, M.; Qureshi, S.; Haase, D.; Alavipanah, S.K., (2019). Automated built-up extraction index: A new technique for mapping surface built-up areas using Landsat 8 OLI imagery. Remote Sens., 11(17): 1966 **(20 pages)**.

Garouani, M.; Amyay, M.; Lahrach, A.; Oulidi, H.J., (2021). Land surface temperature in response to land use/cover change based on remote sensing data and GIS techniques: Application to Saïss Plain, Morocco. J. Ecol. Eng., 22(7): 100-112 (**13 pages**).

Grover, A.; Singh, R.B., (2015). Analysis of urban heat island (UHI) in relation to normalized difference vegetation index (NDVI): A comparative study of Delhi and Mumbai. Environ., 2(4): 125-138 **(14 pages)**.

Guha, S.; Govil, H.; Dey, A.; Gill, N., (2018). Analytical study of land surface temperature with NDVI and NDBI using Landsat 8 OLI and TIRS data in Florence and Naples city, Italy. Eur. J. Remote Sens., 51(1): 667-678 **(12 pages)**.

Himayoun, D.; Roshni, T.; Mohsin, F., (2020). Spatiotemporal variations of land surface temperature and precipitation due to climate change in the Jhelum river basin, India. Musam. 71(4): 661-674 **(14 pages)**.

Hu, S.; Fan, Y.; Zhang, T., (2020). Assessing the effect of land use change on surface runoff in a rapidly urbanized city: A case study of the central area of Beijing. Land. 9(17): 1-15 **(16 pages)**.

Hua, A.K.; Ping, O.W., (2018). The influence of land-use/land-cover changes on land surface temperature: A case study of Kuala Lumpur metropolitan city. Eur. J. Remote Sens., 51(1): 1049-1069 **(21 pages)**.

Ibrahim, G.R.F., (2017). Urban land use land cover changes and their effect on land surface temperature: Case study using Dohuk City in the Kurdistan region of Iraq. Climate, 5(13): **(18 pages)**.

Indarto, I.; Hakim, F.L., (2021). Tracking Land Use Land Cover changes from 2000 to 2018 in a local area of East Java Province, Indonesia. Bull. Geogr. Socio-Eco. Ser., 52(52): 7-24 **(18 pages).**

Jiang, X.; Yang, L.; Tatano, H., (2019). Assessing spatial flood risk from multiple flood sources in a small river basin: A method based on multivariate design rainfall. Water, 11(5): 1031 **(17 pages)**.

Kovář, P.; Vaššová, D.; Janeček, M., (2012). Surface runoff simulation to mitigate the impact of soil erosion, case study of Třebsín (Czech Republic). Soil Water Res., 7(3): 85-96 **(12 pages)**.

Liu, J.; Hagan, D.F.T.; Liu, Y., (2021). Global land surface temperature change (2003-2017) and its relationship with climate drivers: AIRS, MODIS, and ERA5-land based analysis. Remote Sens., 13(1): **(20 pages).**

Mapiam, P.P.; Sharma, A.; Sriwongsitanon, N., (2014). Defining the Z–R relationship using gauge rainfall with coarse temporal resolution: Implications for flood forecasting. J. Hydrologic Eng., 19(8).

Maselli, F., (2012). A method to improve the spatial features of NDVI data series. Eur. J. of Remote Sens., 45(1): 407-420 **(14 pages).**

Mondino, E.B.; Lessio, A.; Gomarasca, M.A., (2016). A fast operative method for NDVI uncertainty estimation and its role in vegetation analysis. Eur. J. of Remote Sens., 49(1): 137-156 **(20 pages)**.

Moslenko, L.; Blagrave, K.; Filazzola, A.; Shuvo, A.; Sharma, S., (2020). Identifying the influence of land cover and human population on chlorophyll a concentrations sing a pseudo-watershed analytical framework. Water, 12(11): 3215 **(21 pages)**.

Mustafa, E.K.; Co, Y.; Liu, G.; Kaloop, M.R.; Beshr, A.A.; Zarzoura, F.; Sadek, M., (2020). Study for predicting land surface temperature (LST) using Landsat data: A comparison of four algorithms. Adv. Civ. Eng., 2020. 1-16: **(16 pages)**.

Neinavaz, E.; Skidmore, A.K.; Darvishzadeh, R., (2020). Effects of prediction accuracy of the proportion of vegetation cover on land surface emissivity and temperature using the NDVI threshold method. Int. J. Appl. Earth Obs. Geoinf., 85: 101984 **(13 pages)**.

Nicolau, R.; David, J.; Caetano, M.; Pereira, J.M.C., (2018). Ratio of land consumption rate to population growth rate–analysis of different formulations applied to mainland Portugal. ISPRS Int. J. Geo-Inf., 8(1): 1-21 **(21 pages)**.

Ozyavuz, M.; Bilgili, B.C.; Silici, A., (2015). Determination of vegetation changes with NDVI method. J. Environ. Prot. Ecol., 16(1): 264-273 **(10 pages)**.

Peng, X.; Wu, W.; Zheng, Y.; Sun, J.; Hu, T.; Wang, P., (2020). Correlation analysis of land surface temperature and topographic

elements in Hangzhou, China, Scientific Reports, Hangzhou, China. Nature, Sci. Rep., 10(1): 10451 **(16 pages)**.

Ranagalage, M.; Estoque, R.C.; Murayama, Y., (2017). An urban heat island study of the Colombo metropolitan area, Sri Lanka, based on Landsat data (1997-2017). ISPRS Int. J. Geo-Inf., 6(7): 189 **(17 pages)**.

Reid, C.E.; Kubzansky, L.D.; Li, J.; Shmool, J.L.; Clougherty, J.E., (2018). It's not easy assessing greenness: A comparison of NDVI datasets and neighborhood types and their associations with self-rated health in New York City. Health Place. 54: 92-101 **(10 pages)**.

Samal, D.R.; Gedam, S.S., (2017). Monitoring land use changes associated with urbanization: An object based image analysis approach. Eur. J. Remote Sens., 48(1): 85-99 **(15 pages).**

Sekertekin, A.; Bonafoni, S., (2020). Land surface temperature retrieval from Landsat 5, 7, and 8 over rural areas: Assessment of different retrieval algorithms and emissivity models and toolbox implementation. Remote Sens., 12(2): 294 **(32 pages)**.

Senanayake, I.P.; Welivitiya, W.D.D.P.; Nadeeka, P.M., (2013). Remote sensing based analysis of urban heat islands with vegetation cover in Colombo city, Sri Lanka using Landsat-7 ETM+ data. Urban Clim., 5: 19-35 (**17 pages**).

Shiraki, Y.; Shigeta, Y., (2013). Effects of land surface temperature on the frequency of convective precipitation in the Tokyo area. J. Geogr. Inf. Sys., 05(3): 303-313 **(11 pages)**.

Stehfest, E.; van Zeist, W.J.; Valin, H.; Havlik, P.; Popp, A.; Kyle, P.; Tabeau, A.; Mason-D'Croz, D.; Hasegawa, T.; Bodirsky, B.L.; Calvin, K.; Doelman, J.C.; Fujimori, S.; Humpenöder, F.; Lotze-Campen, H.; van Meijl, H.; Wiebe, K., (2019). Key determinants of global land-use projections. Nat. Commun., 10(1): 2166 **(10 pages)**.

Turvey, C.G.; McLaurin, M.K., (2012). Applicability of the normalized difference vegetation index (NDVI) in index-based crop insurance design. Weather Clim. Soc., 4(4): 271-284 **(14 pages)**.

USGS, (2019), Landsat 7 (L7) data users' handbook, version 2, 122. United State Geological Survey.

Yuan, F.; Bauer, M.E., (2007). Comparison of impervious surface area and normalized difference vegetation index as indicators of surface urban heat island effects in Landsat imagery. Remote Sens. Environ., 106(3): 375-386 **(12 pages)**.

AUTHOR (S) BIOSKETCHES

Suharyanto, A., Ph.D., Associate Professor, Civil Engineering Department, Universitas Brawijaya, Jl. MT. Haryono 169, Kota Malang, Indonesia.
- Email: *agus.s@ub.ac.id*
- ORCID: 0000-0002-1508-7685
- Web of Science ResearcherID: GWV-8051-2022
- Scopus Author ID: 57211811334
- Homepage: https://sipil.ub.ac.id/

Maulana, A., Ph.D., Professor, Department of Geology, Universitas Hasanuddin, Jl. Poros Malino Km. 6, Gowa, Makassar, Indonesia.
- Email: *adi-maulana@unhas.ac.id*
- ORCID: 0000-0001-9349-0106
- Web of Science ResearcherID: O-7674-2017
- Scopus Author ID: 55912515600
- Homepage: https://eng.unhas.ac.id/geologi/id/dosen/

Suprayogo, D., Ph.D., Professor, Department of Soil Sciences, Universitas Brawijaya, Jl. Veteran, Kota Malang, Indonesia.
- Email: *suprayogo@ub.ac.id*
- ORCID: 0000-0001-5330-3185
- Web of Science ResearcherID: GWZ-7410-2022
- Scopus Author ID: 15754448200
- Homepage: https://tanah.ub.ac.id/

Devia, Y.P., Ph.D., Associate Professor, Civil Engineering Department, Universitas Brawijaya, Jl. MT. Haryono 169, Kota Malang, Indonesia.
- Email: *yatnanta@ub.ac.id*
- ORCID: 0000-0001-8354-3008
- Web of Science ResearcherID: GWZ-7331-2022
- Scopus Author ID: 57200255989
- Homepage: https://sipil.ub.ac.id/

Kurniawan, S., Ph.D., Associate Professor, Department of Soil Sciences, Universitas Brawijaya, Jl. Veteran, Kota Malang, Indonesia.
- Email: *syahrul.fp@ub.ac.id*
- ORCID: 0000-0003-3057-9755
- Web of Science ResearcherID: E-6356-2017
- Scopus Author ID: 55876481800
- Homepage: https://tanah.ub.ac.id/

HOW TO CITE THIS ARTICLE

Suharyanto, A.; Maulana, A.; Suprayogo, D.; Devia, Y.P.; Kurniawan, S., (2023). Land surface temperature changes caused by land cover/ land use properties and their impact on rainfall characteristics. Global J. Environ., Sci. Manage., 9(3): 353-372.

DOI: 10.22035/gjesm.2023.03.01

URL: https://www.gjesm.net/article_696663.html